FULL PAPER

Internal Medicine

Comparison of pancreatic and renal blood flow in a canine tachycardia-induced cardiomyopathy model

Aritada YOSHIMURA[1], Takahiro OHMORI[1], Shusaku YAMADA[1], Takae KAWAGUCHI[1], Miori KISHIMOTO[2], Tomoko IWANAGA[3], Naoki MIURA[3] and Ryuji FUKUSHIMA[1]*

[1]Animal Medical Center, Tokyo University of Agriculture and Technology, Fuchu, Tokyo 183-8509, Japan
[2]Laboratory of Veterinary Imaging, Tokyo University of Agriculture and Technology, Fuchu, Tokyo 183-8509, Japan
[3]Veterinary Teaching Hospital, Kagoshima University, Kagoshima, Kagoshima 890-0065, Japan

ABSTRACT. The pancreas is believed to be vulnerable to hypoperfusion. In dogs with acute pancreatitis, pancreatic ischemia due to heart failure can worsen the condition. However, changes in pancreatic blood flow associated with decreased cardiac function have not been previously studied in dogs. Therefore, we aimed to identify and compare changes in pancreatic versus renal blood flow as a result of cardiac dysfunction. Seven dogs were subjected to rapid ventricular pacing to create heart failure models. Noninvasive blood pressure measurement, ultrasonic cardiography, contrast-enhanced ultrasonography for pancreatic blood flow measurement, and para-aminohippuric acid clearance for renal blood flow measurement were performed before starting and at 2 and 4 weeks after starting the pacing. Left ventricular cardiac output and mean blood pressure decreased at 2 and 4 weeks after starting the pacing, and pancreatic blood flow decreased at 2 and 4 weeks after starting the pacing. However, renal blood flow did not change at 2 weeks but decreased 4 weeks after starting the pacing. Overall, this study demonstrated that reduced pancreatic blood flow due to cardiac dysfunction occurs, similar to renal blood flow. This suggests that decreased pancreatic blood flow is not unusual and may frequently occur in dogs with heart failure. The results of this study support the speculation that heart failure can exacerbate acute pancreatitis. Additionally, this study provides useful basic information for designing further studies to study this association.

KEY WORDS: cardiac output, contrast enhanced ultrasonography, dog, pancreatic blood flow, renal blood flow

Cardiomyopathy, valvular disease, and other forms of heart disease diminish the pumping ability of the heart, ultimately leading to heart failure. Hemodynamic changes associated with heart failure cause hypoperfusion-induced damage to internal organs such as the kidneys, gastrointestinal tract, and liver in a variety of ways [9, 34, 37]. Among these organs, the kidneys are known to be vulnerable to the effects of cardiac dysfunction. Renal hypoperfusion caused by diminished cardiac output is an extremely important factor influencing renal tissue damage and renal dysfunction [34]. In humans and dogs, the association between heart failure and kidney damage is widely known as "cardiorenal syndrome" [30, 34].

Further, among the gastrointestinal organs, the pancreas is also believed to be a vulnerable organ to hypoperfusion in both humans and dogs [14, 42]. According to several experimental reports on rats, pancreatic ischemia has been shown to be an especially important factor in the progression of acute pancreatitis and may lead to fatal pancreatic necrosis [22, 27, 41]. Moreover, decrease in cardiac output and systemic blood pressure are cited as factors causing ischemia [22]. Han *et al.* reported that the concentration of the serum pancreatitis biomarker (canine pancreatic lipase immunoreactivity) is elevated in many dogs with severe congestive heart failure [14]. Therefore, heart failure is expected to be one of the factors that exacerbates acute pancreatitis in dogs.

However, although the association between heart failure and acute pancreatitis is drawing attention, to the best of our knowledge, changes in pancreatic blood flow associated with decreased cardiac function have not been previously verified. Therefore, our objective was to identify changes in pancreatic blood flow as a result of cardiac dysfunction and compare them with changes in renal blood flow (RBF), which has previously been well verified to be associated with decreased cardiac function.

MATERIALS AND METHODS

This study was conducted following the regulations of the Tokyo University of Agriculture and Technology Animal Experiment Committee (approval number 31-2). All experimental animal procedures were performed in compliance with the guidelines outlined in the Guide for the Care and Use of Laboratory Animals (2011).

Animals

In this study, 2 to 3-year-old healthy beagles (three male and four female dogs) weighing 9.2–10.4 kg were included. All of the dogs underwent a general physical examination, blood test, ultrasound examination, x-ray and they were confirmed to be sufficiently healthy for inclusion in this study. The dogs were fed twice daily—at 8 AM and 5 PM—with high-quality feed (Vet's Selection, Yeaster Co., Ltd., Hyogo, Japan) to provide $1.8 \times (70 \times (\text{body weight in kg})^{0.75})$ Kcal/day; water was provided *ad libitum* in stainless steel containers [4]. The dogs were housed in separate rooms maintained at a room temperature and relative humidity of $21 \pm 2°C$ and $50 \pm 20\%$, respectively, with a 12-hr light/dark cycle. The dogs were also allowed to exercise for 30 min once per day.

Creation of a heart failure model

In this study, we used a tachycardia-induced cardiomyopathy model generated by high-frequency electrical stimulation of the ventricles for several weeks to reduce heart function. This model is capable of simulating heart failure and is already widely used as a model of congestive heart failure [44].

The procedures for developing the tachycardia-induced cardiomyopathy model of dogs has been described in detail by Wilson *et al.* [44] and Onogawa *et al.* [31]. Intravenous midazolam (0.2 mg/kg, Dormicum, Maruishi Pharmaceutical Co., Ltd., Osaka, Japan) was administered as an anesthetic premedication. General anesthesia was induced with intravenous propofol (5–6 mg/kg, Fresenius Kabi, Bad Homburg, Germany), and isoflurane (Pfizer, Tokyo, Japan) was administered to maintain anesthesia via an endotracheal tube (end-tidal isoflurane concentration: 1.2–1.7%). The thorax was opened via the 6th intercostal space, and a ventricular stimulation electrode lead (TY216-033, UNIQUE Medical Co., Ltd., Tokyo, Japan) was placed in the right ventricular pericardium. The electrode lead was brought outside the body via a subcutaneous tunnel, and the thorax was closed using the standard method. For pain control, 0.02 mg/kg of intravenous buprenorphine hydrochloride (Lepetan, Otsuka Pharmaceutical Co., Ltd., Tokushima, Japan) was administered preoperatively, and 2 mg/kg of bupivacaine hydrochloride (Marcaine, Aspen Japan, Tokyo, Japan) and 2% lidocaine hydrochloride (Xylocaine, Aspen Japan) were injected intraoperatively at the site of surgery as local anesthetics. Postoperatively, 2 mg/kg robenacoxib (Onsior, Elanco Japan, Tokyo, Japan) was administered subcutaneously on the day of surgery and on the subsequent 3 days. On the day of surgery and the subsequent 7 days, 25 mg/kg intravenous ampicillin sodium (Viccillin, Meiji Seika Pharma Co., Ltd., Tokyo, Japan) was administered for infection control. The dogs were placed in a jacket with a pocket in which an external cardiac pacemaker (EV4543, Taisho Biomed Instruments Co., Ltd., Osaka, Japan) was installed. A period of 14 days post-surgery was reserved for the recovery period. After the recovery period, the electrode leads were connected to the pacemakers, and rapid ventricular pacing (RVP) was initiated; 4 volts of stimulation at a frequency of 260 beats/min was administered.

Experimental protocol

Blood pressure measurement and ultrasonic cardiography (UCG) were conducted pre-RVP and 2 and 4 weeks after starting RVP (baseline, 2W, and 4W). B-mode abdominal ultrasonography (US) was carried out to measure the diameter of major abdominal vessels, contrast-enhanced ultrasonography (CEUS) was used for the quantitative evaluation of pancreatic parenchymal perfusion, and para-aminohippuric acid clearance (C_{PAH}) measurement was used to assess renal perfusion. Blood pressure measurement, UCG, abdominal US, and CEUS were carried out in that order on the same day. Para-aminohippuric acid clearance and blood test were measured on the day after these tests. Examinations at the 2W and 4W time point were carried out 30 min after RVP was suspended temporarily. All investigations were performed in the same order at the same time of day (5–6 PM) after the dogs had been fasting (with *ad libitum* access to drinking water) for ≥12 hr and were sedated with intravenous injection of 0.2 mg/kg butorphanol chloride (Vetorphale, Meiji Seika Pharma Co., Ltd.). The frequency of ventricular pacing was set using an electrocardiograph (D300, Fukuda M-E Kogyo Co., Ltd., Tokyo, Japan). Electrocardiography was also performed daily throughout the study period to confirm accurate pacing.

Blood pressure measurement

Systolic blood pressure (SBP), mean blood pressure (MBP), and diastolic blood pressure (DBP) were measured using a noninvasive oscillometric blood pressure monitor (BP-100D, Fukuda M-E Kogyo Co., Ltd.). The root of the tail was chosen as the measurement site, and a cuff that covered 40–60% of its length was used for this purpose. Measurements were repeated several times, and the mean value of three measurements with an error of ≤3 mmHg was used for each blood pressure parameter.

UCG

Ultrasonic cardiography was performed using an ultrasound unit (Vivid E 95, GE Healthcare Japan Co., Tokyo, Japan) with a 4.0–8.0 MHz sector probe (7S, GE Healthcare Japan Co.). The end-diastolic left ventricular (LV) internal dimension and end-systolic LV internal dimension (LVIDd and LVIDs, respectively) were measured using the M-mode on the right parasternal short-axis view at the level of the tendinous cord. Heart rate (HR) was recorded simultaneously. The LV fractional shortening (FS) was

calculated using the following formula:

FS (%)=([LVIDd −LVIDs]/LVIDd) ×100

Subsequently, the aortic valve orifice was visualized via a left parasternal apical 5-chamber view, and the pre-ejection period (PEP), ejection time (ET), and the ratio of PEP to ET (PEP/ET), an index of LV systolic function, were obtained using the aortic orifice blood flow waveform in the Doppler-mode. The PEP was defined as the time from the Q wave on the electrocardiogram synchronized with echocardiography to the start of blood ejection from the left ventricle. Moreover, the time during which blood was actually ejected from the left ventricle was defined as the ET [7]. Left ventricular cardiac stroke volume (SV) and output (CO) were obtained by the measurement of the aortic diameter (d) and velocity time integral (VTI) based on the LV outflow on pulsed-wave Doppler imaging. The following equations were used:

SV (ml)=(d/2)^2 × π × VTI

CO (l/min)=SV × HR [7]

Ultrasonic cardiography data were measured over an average of nine consecutive beats.

Central venous pressure (CVP) is known to increase with RVP in this animal model; therefore, the range of CVP was assumed to be 5–15 mmHg [20, 31]. Systemic vascular resistance (SVR) in each case was calculated according to the following formula:

SVR (dynes × sec × cm^{-5})=(MBP −CVP)/CO × 79.92 [19]

Body surface area (BSA) and cardiac index (CI) were calculated according to the following formulae:

BSA (m^2)=10.1 × (body weight in g)$^{2/3}$ × 10^{-4} [5]

CI (l × min^{-1} × m^{-2})=CO/BSA [6]

B-mode abdominal US

Abdominal US was carried out using an ultrasound unit (Vivid E 95, GE Healthcare Japan Co.) with an 8.0–11.0 MHz convex probe (8C probe, GE Healthcare Japan Co.).

Animals were held in the supine position, and cross-sectional images of the caudal vena cava (CV), abdominal aorta (Ao), and portal vein (PV) were visualized via the right 11th or 12th intercostal space. The short and long diameters of each vessel were measured, and their mean value was used. Because these vessels are affected by respiration and heartbeat, they were measured at the time of maximum dilation. The ratios of the diameters of the PV and CV to that of the Ao (PV/Ao, CV/Ao) were also calculated.

CEUS

Scanning was conducted with an ultrasound device equipped with a contrast harmonic imaging function (Logiq 7, GE Healthcare Japan Co.) and a 6.0–9.0 MHz linear probe (9L probe, GE Healthcare Japan Co.).

Amplitude modulation was used for the contrast mode. The mechanical index was set at 0.26, a low sound pressure at which microbubbles (MBs) do not break down, and the focus was set immediately below the pancreas. The frame rate was set at 18 Hz. Gain was optimized individually for each animal, and the same value was used for baseline and 2W and 4W scanning. The animals were held in the supine position, and a cross-section of the right lobe of the pancreas running parallel to the duodenum was visualized in B-mode. To visualize the same part of the pancreas each time, the same probe movements were used for each individual animal at baseline and at 2W and 4W. The contrast agent was perflubutane MBs (Sonazoid®, Daiichi-Sankyo Co., Ltd., Tokyo, Japan) which was injected intravenously via a 21 G winged needle previously placed in the cephalic vein. Sonazoid® at a dose of 0.05 ml/kg was diluted in 5 ml of physiological saline according to the previously reported method and injected over a 1-min period using a syringe pump (Top-5300, Top Corp., Tokyo, Japan) [23–25]. A timer was started at the time Sonazoid® entered the body (0 sec). A 300 sec continuous scan of the right lobe of the pancreas was performed while the visualized cross-section was maintained. The continuous images thus obtained were saved as raw video data on the hard disk of the ultrasound scanner.

Pancreatic parenchymal perfusion was quantified on the basis of this saved raw data. Three circular regions of interest (ROIs; 2 mm in diameter) were designated in the pancreatic parenchyma, avoiding blood vessels (Fig. 1). Subsequently, the software that came with the ultrasound scanner was used to measure the intensity (absolute value) in the three ROIs at 5-sec intervals from 0 sec to 180 sec and at 10-sec intervals from 180 sec to 300 sec, and the mean value was calculated. The rate of change in intensity at each time compared to the intensity at 0 sec (relative value) was also calculated. A time-intensity change rate curve (TIC) was then produced. If the position of the pancreas varied due to respiration, the positions of the three ROIs were adjusted manually so that the sites of measurement remained the same. Pancreatic perfusion was quantitatively assessed on the basis of the TIC. The following parameters were calculated: time to peak (TP), time to initial up-slope (TTU), and time to washout (TTW) as time indices, and peak intensity (PI) and the area under

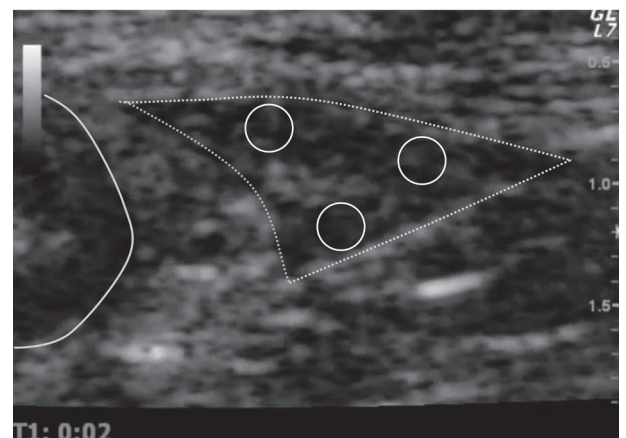

Fig. 1. Positions of three regions of interest set in the right pancreatic lobe parenchyma for contrast-enhanced ultrasonography. The right pancreatic lobe is outlined by a dotted line and the descending duodenum is outlined by a solid line.

the curve (AUC) were used as indices of the increase in intensity (Fig. 2). Time to initial up-slope and TTW were defined as the time taken for the intensity change rate to rise or fall to 30% of the PI.

C_{PAH}

A priming dose of 6 mg/kg of PAH (10% sodium para-aminohippurate injection, Daiichi-Sankyo Co., Ltd., Japan) was injected intravenously via a 22 G needle previously placed in the cephalic vein. To maintain the blood PAH concentration, continuous intravenous infusion of PAH diluted in lactated Ringer's solution was carried out during the experiment at a rate of 3 ml/kg/min (PAH administration rate, 0.4 mg/kg/min). After a PAH equilibration time of 30 min, all of the urine in the bladder was collected via a previously placed 6 Fr urinary balloon catheter to set the baseline condition [36]. Urine samples were subsequently collected three times at 15-min intervals. Furthermore, blood samples were collected at the same time points from the jugular vein using a 22 G injection needle. The volume of urine/min (U_V) was calculated from the volumes of the urine samples. The blood samples were centrifuged at 1,510 g for 10 min, and the hematocrit value (Ht) was calculated after the cellular components and plasma had been obtained.

The PAH concentrations in the plasma samples (P_{PAH}) and urine samples (U_{PAH}) were calculated by using the colorimetric method, as described by Brun & Denmark [3]. The mean values of P_{PAH} and U_{PAH} measured in each of three samples were calculated, and the renal plasma flow (RPF) and RBF were calculated according to the following formulae [36]:

RPF (ml/min)=U_{PAH} / P_{PAH} × U_V
RBF (ml/min)=RPF × 100 / (100−Ht)

Fig. 2. Schematic diagram of a typical time-intensity change rate curve (TIC) showing the measured parameters. The intensity at the beginning of scanning was treated as the baseline intensity, and the rate of change in intensity at each time point was plotted to generate the TIC. Time to peak (TP) is the time taken to reach peak intensity (PI). The time to initial up-slope (TTU) is the time taken to reach 30% of the PI for the first time, and the time to washout (TTW) is the time taken to reach 30% of the PI for the first time after the PI has been achieved. The area under the curve (AUC) indicates the area formed between the TIC and the baseline intensity.

Blood test

Blood samples were collected from the jugular vein in a tube with serum or plasma-separating medium and centrifuged at 1,510 g for 10 min. Measurement of the concentration of serum canine pancreatic lipase immunoreactivity (cPLI: reference range ≤200 μg/l), which is a biomarker of pancreatic acinar cell injury, was performed by a commercial laboratory (IDEXX Laboratories, K. K., Tokyo, Japan) [43]. Measurement of the concentration of serum symmetric dimethylarginine (SDMA: reference range ≤14 μg/dl), which is a biomarker of renal function, was also performed by a commercial laboratory (IDEXX Laboratories, K. K.) [13, 29]. Both cPLI and SDMA were measured using an enzyme immunoassay. Plasma was separated and used for the measurement of blood urea nitrogen (BUN: reference range 9.2–29.0 mg/dl) and creatinine (Cre: reference range 0.4–1.4 mg/dl) levels by using a biochemical analyzer suitable for animal samples (Fuji DRI-CHEM 7000 V, FUJIFILM Medical Co., Ltd., Tokyo, Japan).

Statistical analysis

The intensity change rates during each time of the TIC of the pancreatic parenchyma are expressed as the mean ± standard error. All other data are expressed as the mean ± standard deviation. All data were tested for normality using the Shapiro-Wilk test. Blood pressure, UCG parameters, abdominal US parameters, CEUS parameters other than the intensity change rate, C_{PAH} values, and blood test values at baseline and after 2W and 4W were compared by conducting a one-way analysis of variance (ANOVA) with post-hoc multiple comparisons using a Bonferroni correction. The intensity change rates during each time at baseline and after 2W and 4W were compared using the Friedman test with post-hoc multiple comparisons using a Scheffe's method. The statistical analyses were performed using statistical software (BellCurve for Excel, Social Survey Research Information Co., Ltd., Tokyo, Japan). For all tests, P<0.05 was considered to be statistically significant.

RESULTS

Throughout the study period (4 weeks), RVP was not observed to cause any clinical symptoms such as loss of appetite, cough, gastrointestinal symptoms, or respiratory distress in any of the animals.

Blood pressure measurement

Systolic blood pressure, MBP, and DBP were significantly lower at 2W and 4W than at baseline (DBP, P<0.05; others, P<0.01). There were no significant differences between the values at 2W or 4W (Table 1). Assuming a CVP value of 5 mmHg at baseline, of 10, or 15 mmHg at 2W and 4W, there were no significant differences in SVR between baseline, 2W, or 4W, for all combinations (Table 2).
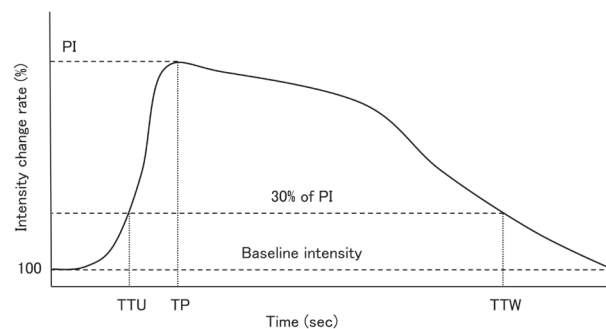
UCG

The LV fractional shortening (both *P*<0.01), SV (baseline vs. 2W, *P*<0.05; baseline vs. 4W, *P*<0.01), CO (both *P*<0.05), and CI (both *P*<0.01) were significantly lower at 2W and 4W than at baseline. Furthermore, FS was significantly lower at 4W than at 2W (*P*<0.05). The end-diastolic LV internal dimension, LVIDs, and PEP/ET were significantly higher at 2W and 4W than at baseline (all *P*<0.01) (Table 1). However, except for FS, none of these parameters showed significant differences between 2W and 4W.

B-mode US

There were no significant differences in PV/Ao between any of the time points (Table 1). However, CV/Ao at 2W tended to be larger and that at 4W was significantly larger (*P*<0.05) than at baseline (Table 1).

CEUS

Peak intensity and the AUC were significantly lower at 2W and 4W than at baseline (both *P*<0.01). Moreover, TP was significantly longer at 2W and 4W than at baseline (baseline vs. 2W, *P*<0.05; baseline vs. 4W, *P*<0.01). There were no significant differences between 2W and 4W, and there were no significant differences between TTU and TTW at any time point (Table 3). The intensity change rate from 20 sec to 125 sec and 240 sec after Sonazoid® injection was significantly lower at 2W and 4W than at baseline. From 130 sec to 140 sec, the intensity change rate was significantly lower at 4W than at baseline. At 250 sec and 270 sec, the intensity change rate was significantly lower at 2W than at baseline time point. There were no significant differences between 2W and 4W (Figs. 3 and 4).

C$_{PAH}$

There was no significant difference in RPF or RBF between 2W and baseline; however, at 4W, both showed a significant decrease compared to baseline (RPF, *P*<0.05; RBF, *P*<0.01) (Table 4).

Table 1. Values of ultrasonic cardiography, B-mode abdominal ultrasonography, and blood pressure measurement

	Baseline	2W	4W
HR (bpm)	107 ± 14	115 ± 36	142 ± 23
LVIDd (mm)	31.1 ± 2.8	39.4 ± 3.0[b]	40.3 ± 3.1[b]
LVIDs (mm)	19.2 ± 2.7	33.2 ± 3.3[b]	36.0 ± 2.3[b]
FS (%)	38.5 ± 5.2	16.2 ± 3.1[b]	10.7 ± 2.3[b,c]
PEP/ET	0.3 ± 0.0	0.5 ± 0.0[b]	0.6 ± 0.0[b]
SV (m*l*)	18.8 ± 2.9	13.3 ± 2.1[a]	10.9 ± 2.3[b]
CO (*l*/min)	2.1 ± 0.2	1.6 ± 0.4[a]	1.5 ± 0.3[a]
CI (*l*/min/m^2)	4.4 ± 0.5	3.4 ± 0.9[b]	3.2 ± 0.8[b]
SBP (mmHg)	151.2 ± 20.2	116.1 ± 16.6[b]	105.0 ± 11.8[b]
MBP (mmHg)	102.7 ± 8.8	79.0 ± 12.1[b]	74.0 ± 10.2[b]
DBP (mmHg)	80.2 ± 6.8	62.7 ± 11.0[a]	58.6 ± 10.4[a]
CV/Ao	1.1 ± 0.2	1.4 ± 0.3	1.5 ± 0.4[a]
PV/Ao	1.0 ± 0.1	1.1 ± 0.2	1.0 ± 0.1

All values are expressed as a mean ± standard deviation. HR, heart rate; LVIDd, end-diastolic left ventricular internal dimension; LVIDs, end-systolic left ventricular internal dimension; FS, left ventricular fractional shortening; PEP/ET, pre-ejection period/ejection time of the left ventricle; SV, left ventricular stroke volume; CO, left ventricular cardiac output; CI, cardiac index; SBP, systolic blood pressure; MBP, mean blood pressure; DBP, diastolic blood pressure; CV/Ao, caudal vena cava-to-abdominal aorta root ratio; PV/Ao, portal vein-to-abdominal aorta root ratio; baseline, before the initiation of rapid ventricular pacing; 2W, 2 weeks after the initiation of rapid ventricular pacing; 4W, 4 weeks after the initiation of rapid ventricular pacing. a) *P*<0.05 versus baseline; b) *P*<0.01 versus baseline; c) *P*<0.05 versus 2W.

Table 2. Systemic vascular resistance when central venous pressure is postulated to be 5 to 15 mmHg

	mmHg	Period		
		Baseline	2W	4W
SVR (dynes×sec×cm^{-5})	5	3,712 ± 606	3,911 ± 1,277	3,890 ± 1,389
	10	3,522 ± 589	3,648 ± 1,233	3,613 ± 1,321
	15	3,333 ± 573	3,386 ± 1,170	3,336 ± 1,253

All values are expressed as a mean ± standard deviation. SVR, systemic vascular resistance; Baseline, before the initiation of rapid ventricular pacing; 2W, 2 weeks after the initiation of rapid ventricular pacing; 4W, 4 weeks after the initiation of rapid ventricular pacing.

Table 3. Values of parameters of the time-intensity change rate curve in the contrast-enhanced ultrasonography of the pancreatic parenchyma

	Baseline	2W	4W
PI (%)	113.3 ± 4.6	108.2 ± 2.9[b]	107.3 ± 3.1[b]
AUC	369.7 ± 129.0	198.5 ± 110.5[b]	188.7 ± 99.7[b]
TP (sec)	55.7 ± 18.4	104.3 ± 30.4[a]	104.4 ± 32.5[b]
TTU (sec)	19.3 ± 5.0	32.9 ± 18.5	33.6 ± 16.8
TTW (sec)	232.9 ± 57.3	200.0 ± 53.9	227.9 ± 55.3

All values are expressed as a mean ± standard deviation. PI, peak intensity; AUC, area under the curve; TP, time to peak; TTU, time to initial up-slope, TTW, time to washout; baseline, before the initiation of rapid ventricular pacing; 2W, 2 weeks after the initiation of rapid ventricular pacing; 4W, 4 weeks after the initiation of rapid ventricular pacing. a) $P<0.05$ versus baseline. b) $P<0.01$ versus baseline.
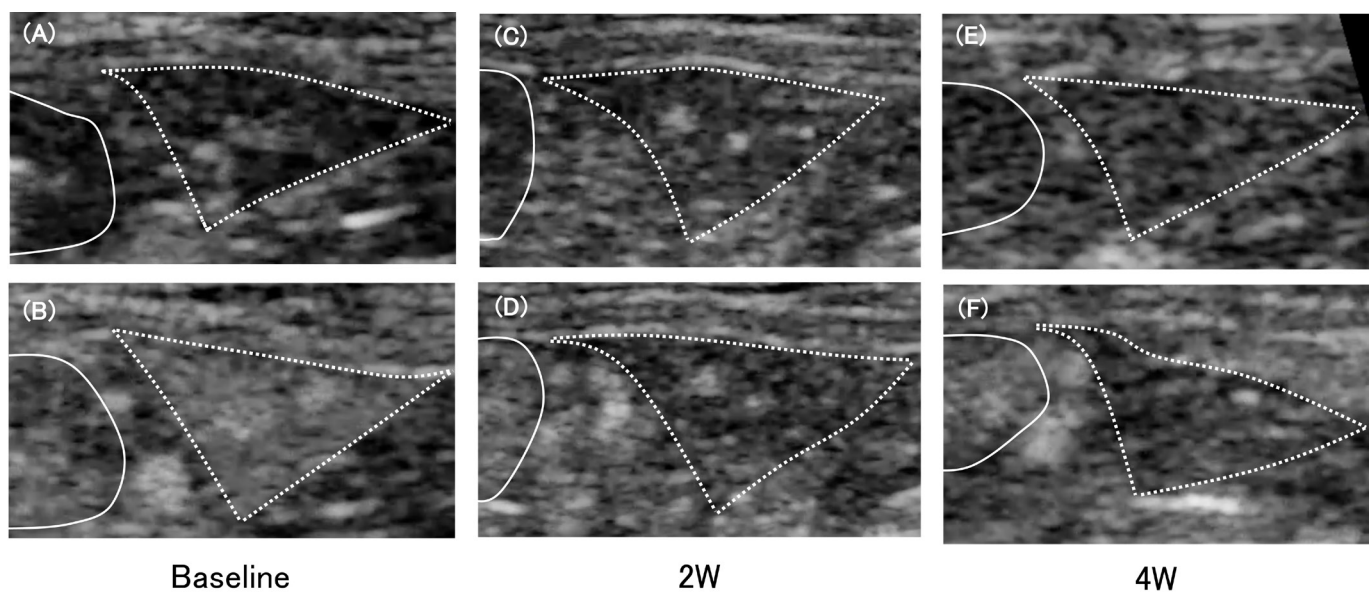

Fig. 3. Representative contrast-enhanced ultrasonography images of the transverse view of the right pancreatic lobe (outlined by dotted lines) and the descending duodenum (outlined by solid lines). (A) and (B) show changes over time following contrast-agent administration before starting rapid ventricular pacing (baseline). (A): Immediately after administration; (B): at maximum intensity. (C) and (D) show changes over time following contrast-agent administration at 2 weeks (2W) after starting rapid ventricular pacing. (C): Immediately after administration; (D): at maximum intensity. (E) and (F) show changes over time following contrast-agent administration at 4 weeks (4W) after starting rapid ventricular pacing. (E): Immediately after administration; (F): at maximum intensity. The increase in intensity at 2W and 4W was less pronounced than that at baseline.

Blood test

There were no significant differences in serum cPLI and SDMA concentrations, or plasma BUN and Cre concentrations between any of the time points (Table 5). All parameters were within the reference ranges.

DISCUSSION

In this study, cardiac, function and blood pressure in a canine tachycardia-induced cardiomyopathy model, in which RVP was conducted for 4 weeks, decreased significantly from 2W. Pancreatic blood flow quantified by CEUS also decreased significantly from 2W. There was no significant difference in RBF measured by C_{PAH} at 2W, although a significant decrease was evident at 4W.

Cardiac function assessed using UCG at 2W and 4W revealed decreased FS and increased PEP/ET for the left ventricle. Normally, a reduction in FS is caused by decreased preload, increased afterload, or reduced cardiac contractility [28]. In this study, LVIDd was used as an index of preload, and SVR was used as an index of afterload. The end-diastolic LV internal dimension was significantly increased by RVP. Central venous pressure is included in the formula to calculate SVR. Therefore, SVR will be affected by the CVP. Central venous pressure is known to increase from 5 before stimulation to around 10 mmHg with RVP in dogs created in the same way used in this study [31]. Therefore, in this study, CVP was postulated to be 5 mmHg at baseline and to be 10 or 15 mmHg at 2W and 4W. As a result, substituting these values as CVP values, there was no significant difference in SVR between baseline, 2 W, and 4 W for all combinations. Therefore, the decrease in FS is considered to indicate a decrease in cardiac
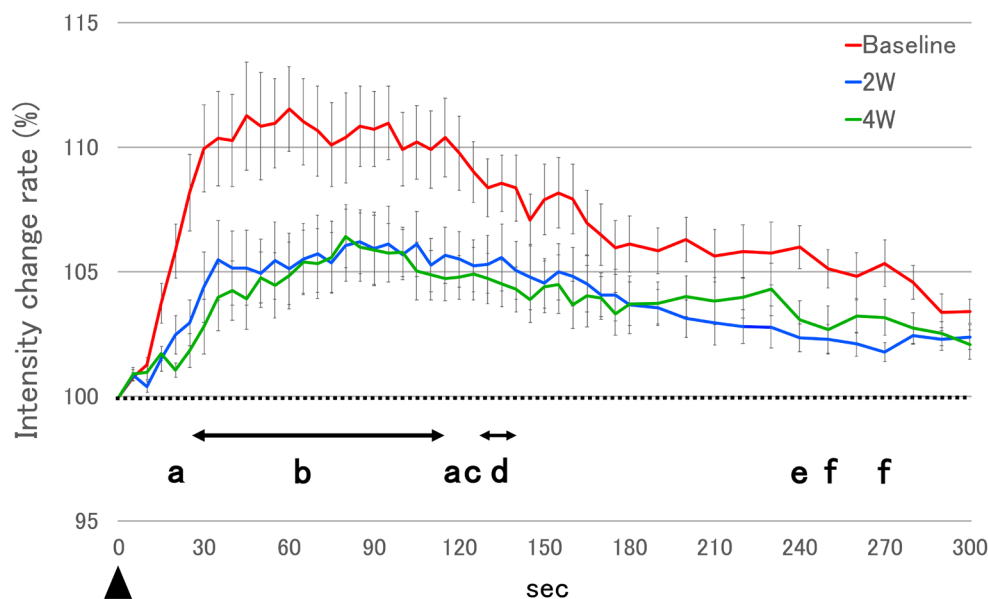
Fig. 4. Time-intensity change rate curve created using contrast-enhanced ultrasonography. The intensity before the administration of contrast agents is defined as 100% (dotted line). The intensity change rate at each time point is shown as the mean ± standard error. The red solid line indicates baseline, blue indicates 2W, and green indicates 4W. Black arrowhead, administration of contrast agents; baseline, before the initiation of rapid ventricular pacing; 2W, 2 weeks after the initiation of rapid ventricular pacing; 4W, 4 weeks after the initiation of rapid ventricular pacing; a, $P<0.05$ baseline versus 2W and $P<0.01$ baseline versus 4W; b, $P<0.01$ baseline versus 2W and baseline versus 4W; c, $P<0.05$ baseline versus 2W and baseline versus 4W; d, $P<0.05$ baseline versus 4W; e, $P<0.01$ baseline versus 2W and $P<0.05$ baseline versus 4W; f, $P<0.05$ baseline versus 2W.

Table 4. Renal plasma flow and renal blood flow in para-aminohippuric acid clearance

	Baseline	2W	4W
RPF (ml/min)	101.2 ± 26.4	97.4 ± 24.2	78.7 ± 20.4[a)]
RBF (ml/min)	191.3 ± 60.0	165.9 ± 48.6	132.4 ± 43.9[b)]

All values are expressed as a mean ± standard deviation. RPF, renal plasma flow; RBF, renal blood flow; baseline, before the initiation of rapid ventricular pacing; 2W, 2 weeks after the initiation of rapid ventricular pacing; 4W, 4 weeks after the initiation of rapid ventricular pacing. a) $P<0.05$ versus baseline. b) $P<0.01$ versus baseline.

Table 5. Values of blood test

	Baseline	2W	4W
cPLI (μg/l)	31.4 ± 3.5	33.9 ± 9.4	54.0 ± 30.3
SDMA (μg/dl)	7.3 ± 1.7	8.4 ± 1.3	9.8 ± 2.9
BUN (mg/dl)	11.0 ± 3.2	17.1 ± 3.6	15.6 ± 4.4
CRE (mg/dl)	0.7 ± 0.3	0.7 ± 0.1	0.6 ± 0.2

All values are expressed as a mean ± standard deviation. cPLI, canine pancreatic lipase immunoreactivity; SDMA, symmetric dimethylarginine; BUN, blood urea nitrogen; CRE, creatinine; baseline, before the initiation of rapid ventricular pacing; 2W, 2 weeks after the initiation of rapid ventricular pacing; 4W, 4 weeks after the initiation of rapid ventricular pacing.

contractility. Moreover, a higher PEP/ET value indicates that cardiac contractility is lower and vice versa [7]. The ratio of PEP to ET was significantly increased by RVP in this study. The changes in these two parameters, FS and PEP/ET, indicate that systolic function in the left ventricle of the model animals had declined from its baseline level as a result of RVP.

We also observed decreases in the SV and CO of the left ventricle of the model animals, which may have been due to the diminished systolic function of the left ventricle. Because the experimental animals used in this study were confined to cages most of the time, they did not exhibit obvious symptoms of heart failure. However, CI with individual variation in CO corrected by BSA was below the reference range for healthy dogs (3.5–5.5 $l/min/m^2$) at 2W [15]. This low CI value indicates that the experimental animals were hemodynamically experiencing heart failure. These dogs were, therefore, considered to be suitable models of heart failure for this study.

Contrast-enhanced ultrasonography enables the assessment of perfusion status of particular organs or lesions over time and quantitively, via the creation of a TIC based on changes in the intensity of a contrast agent over time [11, 17, 18, 23–26]. Microbubbles are used as contrast agents because they strongly reflect ultrasound and increase the echogenicity of fine capillary vessel networks. In particular, Sonazoid® is a low sound-pressure contrast agent that is resistant to disruption, and it can therefore be observed over long periods [16]. Because the MBs are rapidly destroyed by exposure to high-pressure ultrasound, they can be used for repeated tests. Because of these characteristics, they are widely used for evaluating organ perfusion [11, 18, 23–25].

In this study, in the TIC for the pancreatic parenchyma, both PI and the AUC were significantly lower at 2W and 4W than at

baseline. Peak intensity indicates the maximum flow of MBs in the ROI, whereas the AUC indicates the total quantity of MBs entering the ROI during the observation period [11, 17, 26]. The decreases in PI and the AUC of the pancreatic parenchyma thus signify decreased blood flow volume in the pancreas during the observation period. In the TICs corresponding to 2W and 4W, the increase in intensity decreased significantly from 20 sec to 125 sec after intravenous MB injection during all time points relative to that corresponding to baseline. These time points correspond to the phases at which the intensity of the pancreatic parenchyma starts to increase and reaches its peak or plateau, and in human medicine, the period of increased intensity, including the peak, is considered to reflect the arterial phase [26]. Moreover, there is no apparent difference in the shape of TICs between humans and dogs [17, 23, 26]. For this reason, in this model (i.e., in dogs), the decrease in pancreatic parenchymal blood flow, which was suggested to occur at 2W and 4W by our results, was considered to have been caused by reduced arterial blood flow. All of the blood pressure parameters (SBP, MBP, and DBP) also decreased significantly. Among these, MBP in particular is an index of the driving pressure necessary for the organs to be perfused with blood [21]. The absence of any decrease in SVR suggests that the decrease in MBP seen in the experimental animals in this study was mainly caused by the decrease in CO. We therefore concluded that the decrease in pancreatic parenchymal blood flow observed in the experimental animals in this study was due to a decrease in CO. Time to peak was also more delayed in the TICs at 2W and 4W than at baseline. A delay in TP indicates a decline in the MB flow velocity, which means that not only the volume of arterial blood, but also its flow velocity, decreased.

At almost all of the time points later than 125 sec after intravenous Sonazoid® injection, there was no significant difference in the rate of change in intensity between 2W and baseline and between 4W and baseline. This decrease in intensity is believed to mainly reflect the venous phase [26], and it expresses the washout of MBs from the ROIs. Therefore, if there is congestion in the venous system in the pancreas, specifically in the PV, the decrease in intensity will be more gradual [24, 25]. Right atrial pressure is considered to be the most sensitive index for assessing venous congestion in systemic circulation. Ultrasound measurement of the diameter of the CV is a widely used noninvasive method for evaluating right atrial pressure [32]. The structural characteristics of the hepatic vein, which lacks valves, indicate that elevated right atrial pressure is passively disseminated to the PV. This means that elevated right atrial pressure causes congestion and dilation of the PV [33]. In this study, the absence of any significant difference in the diameter of the PV indicates that there were no findings strongly suggestive of pancreatic congestion. In the TICs, there was no significant difference in TTW, which may be an index of venous flow velocity. Therefore, at least in the heart failure model used in this study, the decreased pancreatic blood flow that was observed was more due to decreased arterial blood flow to the pancreas than due to the effect of congestion of the pancreatic venous system.

Unlike the observed changes in pancreatic blood flow, there was no significant change in RBF measured by C_{PAH} at 2W relative to that at baseline. This may be partly due to the kidney's high capacity to self-regulate blood flow. Even in the event of decreased renal perfusion pressure due to cardiac dysfunction, dehydration, hemorrhage, or other causes, as long as MBP does not decrease by approximately >80 mmHg, the kidneys are capable of maintaining total RBF and glomerular capillary blood pressure by dilating afferent arterioles and contracting efferent venules [1]. Subsequently, RBF at 4W was significantly lower than that at baseline. In this study, the diameter of the CV at 2W did not differ significantly from its baseline diameter, but at 4W it was dilated. This suggested that right atrial pressure was elevated. Rapid ventricular pacing is known to cause contractile dysfunction of both ventricles, and cause an increase in the biventricular end-diastolic and biatrial pressure [31, 44]. Elevated right atrial pressure increases renal venous pressure and causes renal congestion [8]. Because the kidneys are enclosed in a capsule, renal congestion increases renal interstitial pressure, further fueling renal hypoperfusion [45]. Therefore, the decrease in RBF at 4W may have been due to not only the decrease in MBP owing to reduced CO, but also renal congestion. In this study, the maximum CV diameter was used as an index for estimating increases in right atrial pressure. In humans, the inferior vena cava diameter is known to vary with respiration, and is smallest during inspiration and largest during expiration [10]. The respiratory variation decreases as right atrial pressure increases. Hence, in human medicine, the accuracy of right atrial pressure estimation is further improved by combining the inferior vena cava collapsibility index, which quantifies respiratory variability, as well as measuring the maximum inferior vena cava diameter [35]. Therefore, we may have been able to capture an increase in right atrial pressure in RVP in dogs at an earlier stage by simultaneously measuring the maximal CV diameter and the collapsibility index.

In this study, there was no significant change in serum SDMA concentration at 4W. SDMA is a useful biomarker for estimating the glomerular filtration rate, and has been shown to be more sensitive than Cre in evaluating renal function [13, 29]. However, the serum SDMA concentration increases when the glomerular filtration rate decreases by 40% on average [13, 29]. Therefore, these model animals are considered to have retained the renal function to maintain homeostasis. However, even if mild renal dysfunction occurred, it may not have been detected.

Kyogoku *et al.* reported that pancreatic ischemia in rats with experimentally induced acute pancreatitis caused progression to fatal severe pancreatitis [22]. Moreover, they described decreases in cardiac output and systemic blood pressure as causes of ischemia and stressed the importance of maintaining systemic circulation and intra-pancreatic hemodynamics to prevent progression to severe acute pancreatitis [22]. Han *et al.* reported that the concentration of the serum pancreatitis biomarker (canine pancreatic lipase immunoreactivity) is elevated in many dogs with severe congestive heart failure and cited pancreatic hypoperfusion as the main factor [14]. Therefore, it is speculated that heart failure causes decreased pancreatic blood flow, increasing the severity of acute pancreatitis. In this study, there was no significant change in serum cPLI concentration, which is considered to reflect pancreatic acinar cell injury [43]. However, Trivedi *et al.* reported that the sensitivity of cPLI in dogs with mild histological pancreatitis is as low as 21–43% [43]. Therefore, it is necessary to consider the possibility that mild pancreatic acinar cell injury due to pancreatic hypoperfusion could not be detected in this study [43]. Thus, in order to verify whether heart failure can cause pancreatic injury in this model, it is necessary to carry out further studies including histopathological diagnosis.

This study has several limitations. First, different methods were used to measure blood flow in the pancreas and kidneys. Contrast-enhanced ultrasonography has been used in human and veterinary medicine as a noninvasive method for measuring organ blood flow without anesthesia [11, 18, 23–25]. Several detailed methods for measuring pancreatic blood flow in dogs, using Sonazoid® as an ultrasound contrast agent, have been reported [23–25]. On the other hand, although the usefulness of CEUS has also been reported in the measurement of RBF [11, 38], there has previously been no report of evaluating RBF in dogs using Sonazoid®. Para-aminohippuric acid is filtered from the glomeruli and secreted from the urinary tubules, and it is not reabsorbed. Because blood passing through these excretory regions of the renal parenchyma accounts for 90% of the blood flowing through the kidneys, C_{PAH} is still regarded as the gold standard for measuring RBF [12]. Therefore, we decided to use C_{PAH} instead of CEUS to evaluate RBF in this study. We observed a decrease in RBF using C_{PAH} as an index at 4W. However, since the difference in the detection sensitivity of RBF between C_{PAH} and CEUS has not been examined, it is necessary to pay attention to simply comparing the temporal differences in the decreases in pancreatic blood flow and RBF. The second limitation was that the ROIs for CEUS comprised only 3 sites in the right lobe of the pancreas, that is, we evaluated blood flow in only one part of the pancreas. We chose this location because the right lobe of the pancreas is more easily visualized than other parts by ultrasound in dogs. Takeda *et al.* carried out perfusion computerized tomography of the pancreas in healthy humans and stated that there was no difference in blood flow among the different parts of the pancreas (head, body, and tail); they also suggested that any lesional site in the pancreas is comparable to healthy pancreatic tissue [40]. The third limitation was that we induced heart failure in young, healthy dogs over a short period (4 weeks). The heart failure model animals used in this study are RVP dogs exhibiting hemodynamics similar to dilated cardiomyopathy [39]. On the other hand, the most frequently encountered type of heart disease in dogs in a clinical setting is mitral regurgitation due to mitral myxomatous degeneration, which is seen in middle to old age. In addition, mitral regurgitation has relatively maintained contractility until late in its disease state [2]. Caution is therefore required when directly extrapolating our results to the hemodynamics of dogs with chronic heart failure. The fourth limitation was that a non-invasive blood pressure measurement was adopted. Therefore, it is necessary to consider the possibility that non-invasive measurements may not capture dynamic and real-time blood pressure changes, compared to invasive blood pressure measurements, which are considered the gold standard for blood pressure measurements. Finally, our study included only a small number of animals.

In conclusion, this study demonstrated that reduced pancreatic blood flow due to cardiac dysfunction occurs, similar to RBF. The results of this study support the speculation that heart failure can be an exacerbating factor for acute pancreatitis. Additionally, this study will provide useful basic information to help design further studies in this field.

REFERENCES

1. Abuelo, J. G. 2007. Normotensive ischemic acute renal failure. *N. Engl. J. Med.* **357**: 797–805. [Medline] [CrossRef]
2. Atkins, C., Bonagura, J., Ettinger, S., Fox, P., Gordon, S., Haggstrom, J., Hamlin, R., Keene, B., Luis-Fuentes, V. and Stepien, R. 2009. Guidelines for the diagnosis and treatment of canine chronic valvular heart disease. *J. Vet. Intern. Med.* **23**: 1142–1150. [Medline] [CrossRef]
3. Brun, C. 1951. A rapid method for the determination of para-aminohippuric acid in kidney function tests. *J. Lab. Clin. Med.* **37**: 955–958. [Medline]
4. Crane, W. S., Griffin, W. R. and Messent, R. P. 2000. Introduction to commercial pet foods. pp. 111–126. *In*: Small Animal Clinical Nutrition, 4th ed. (Thatcher, D. C., Remillard, L. R. and Roudebush, P. eds.), Mark Morris Institute Hand, Kansas.
5. della Torre, P. K., Kirby, A. C., Church, D. B. and Malik, R. 2000. Echocardiographic measurements in greyhounds, whippets and Italian greyhounds--dogs with a similar conformation but different size. *Aust. Vet. J.* **78**: 49–55. [Medline] [CrossRef]
6. Dell'Italia, L. J., Starling, M. R., Blumhardt, R., Lasher, J. C. and O'Rourke, R. A. 1985. Comparative effects of volume loading, dobutamine, and nitroprusside in patients with predominant right ventricular infarction. *Circulation* **72**: 1327–1335. [Medline] [CrossRef]
7. Feigenbaum, H. 1986. Echocardiographic evaluation of cardiac chambers. pp. 127–187. *In*: Echocardiography, 4th ed. (Feigenbaum, H. ed.), Lea & Febiger, Philadelphia.
8. F Gnanaraj, J., von Haehling, S., Anker, S. D., Raj, D. S. and Radhakrishnan, J. 2013. The relevance of congestion in the cardio-renal syndrome. *Kidney Int.* **83**: 384–391. [Medline] [CrossRef]
9. Fouad, Y. M. and Yehia, R. 2014. Hepato-cardiac disorders. *World J. Hepatol.* **6**: 41–54. [Medline] [CrossRef]
10. Grant, E., Rendano, F., Sevinc, E., Gammelgaard, J., Holm, H. H. and Grønvall, S. 1980. Normal inferior vena cava: caliber changes observed by dynamic ultrasound. *AJR Am. J. Roentgenol.* **135**: 335–338. [Medline] [CrossRef]
11. Haers, H., Daminet, S., Smets, P. M. Y., Duchateau, L., Aresu, L. and Saunders, J. H. 2013. Use of quantitative contrast-enhanced ultrasonography to detect diffuse renal changes in Beagles with iatrogenic hypercortisolism. *Am. J. Vet. Res.* **74**: 70–77. [Medline] [CrossRef]
12. Hall, E. J. 2011. Urine Formation by the Kidneys: II. Tubular Reabsorption and Secretion. pp. 323–343. *In*: Guyton and Hall Textbook of Medical Physiology, 12th ed. (Hall, E. J. ed.), Elsevier, Philadelphia.
13. Hall, J. A., Yerramilli, M., Obare, E., Yerramilli, M., Almes, K. and Jewell, D. E. 2016. Serum concentrations of symmetric dimethylarginine and creatinine in dogs with naturally occurring chronic kidney disease. *J. Vet. Intern. Med.* **30**: 794–802. [Medline] [CrossRef]
14. Han, D., Choi, R. and Hyun, C. 2015. Canine pancreatic-specific lipase concentrations in dogs with heart failure and chronic mitral valvular insufficiency. *J. Vet. Intern. Med.* **29**: 180–183. [Medline] [CrossRef]
15. Haskins, S. C. 1999. Treatment of shock. pp. 272–290. *In*: Textbook of Canine and Feline Cardiology: Principle and Clinical Practice, 2nd ed. (Fox, P. R., Sisson, D. and Moise, N. S. eds.), W. B. Saunders Company, Philadelphia.
16. Hatanaka, K., Kudo, M., Minami, Y., Ueda, T., Tatsumi, C., Kitai, S., Takahashi, S., Inoue, T., Hagiwara, S., Chung, H., Ueshima, K. and Maekawa, K. 2008. Differential diagnosis of hepatic tumors: value of contrast-enhanced harmonic sonography using the newly developed contrast agent, Sonazoid. *Intervirology* **51** Suppl 1: 61–69. [Medline] [CrossRef]
17. Kersting, S., Konopke, R., Kersting, F., Volk, A., Distler, M., Bergert, H., Saeger, H. D., Grützmann, R. and Bunk, A. 2009. Quantitative perfusion

analysis of transabdominal contrast-enhanced ultrasonography of pancreatic masses and carcinomas. *Gastroenterology* **137**: 1903–1911. [Medline] [CrossRef]

18. Kersting, S., Ludwig, S., Ehehalt, F., Volk, A. and Bunk, A. 2013. Contrast-enhanced ultrasonography in pancreas transplantation. *Transplantation* **95**: 209–214. [Medline] [CrossRef]

19. Kishikawa, K., Namiki, A. and Iwasaki, H. 1989. The cardiovascular effects of naloxone administration after fentanyl anesthesia in hypercapnic patients. *J. Anesth.* **3**: 48–53. [Medline] [CrossRef]

20. Kittleson, M. D. and Kienle, R. D. 1998. Pulmonary arterial and systemic arterial hypertension. pp. 523–542. *In*: Small Animal Cardiovascular Medicine. (Kittleson, M. D. and Kienle, R. D. eds.), Mosby, St Louis.

21. Klabunde, R. E. 2012. Vascular function. pp. 93–123. *In*: Cardiovascular Physiology Concepts, 2nd ed.(Klabunde, R. E. ed.), Lippincott Williams & Wilkins, Philadelphia.

22. Kyogoku, T., Manabe, T. and Tobe, T. 1992. Role of ischemia in acute pancreatitis. Hemorrhagic shock converts edematous pancreatitis to hemorrhagic pancreatitis in rats. *Dig. Dis. Sci.* **37**: 1409–1417. [Medline] [CrossRef]

23. Lim, S. Y., Nakamura, K., Morishita, K., Sasaki, N., Murakami, M., Osuga, T., Ohta, H., Yamasaki, M. and Takiguchi, M. 2013. Qualitative and quantitative contrast enhanced ultrasonography of the pancreas using bolus injection and continuous infusion methods in normal dogs. *J. Vet. Med. Sci.* **75**: 1601–1607. [Medline] [CrossRef]

24. Lim, S. Y., Nakamura, K., Morishita, K., Sasaki, N., Murakami, M., Osuga, T., Ohta, H., Yamasaki, M. and Takiguchi, M. 2014. Qualitative and quantitative contrast-enhanced ultrasonographic assessment of cerulein-induced acute pancreatitis in dogs. *J. Vet. Intern. Med.* **28**: 496–503. [Medline] [CrossRef]

25. Lim, S. Y., Nakamura, K., Morishita, K., Sasaki, N., Murakami, M., Osuga, T., Yokoyama, N., Ohta, H., Yamasaki, M. and Takiguchi, M. 2015. Quantitative contrast-enhanced ultrasonographic assessment of naturally occurring pancreatitis in dogs. *J. Vet. Intern. Med.* **29**: 71–78. [Medline] [CrossRef]

26. Matsubara, H., Hirooka, Y., Itoh, A., Kawashima, H., Ohno, E., Ishikawa, T., Ito, Y., Nakamura, Y., Hiramatsu, T., Nakamura, M., Miyahara, R., Ohmiya, N. and Goto, H. 2011. Quantitative analysis of pancreatic disorders using contrast-enhanced endoscopic ultrasonography. *Suizo* **26**: 6–10. [CrossRef]

27. Mithöfer, K., Fernández-del Castillo, C., Frick, T. W., Foitzik, T., Bassi, D. G., Lewandrowski, K. B., Rattner, D. W. and Warshaw, A. L. 1995. Increased intrapancreatic trypsinogen activation in ischemia-induced experimental pancreatitis. *Ann. Surg.* **221**: 364–371. [Medline] [CrossRef]

28. Moise, N. S. and Fox, P. R. 1999. Echocardiography and doppler imaging. pp. 131–171. *In*: Textbook of Canine and Feline Cardiology: Principle and Clinical Practice, 2nd ed. (Fox, P. R., Sisson, D. and Moise, N. S. eds.), W. B. Saunders Company, Philadelphia.

29. Nabity, M. B., Lees, G. E., Boggess, M. M., Yerramilli, M., Obare, E., Yerramilli, M., Rakitin, A., Aguiar, J. and Relford, R. 2015. Symmetric dimethylarginine assay validation, stability, and evaluation as a marker for early detection of chronic kidney disease in dogs. *J. Vet. Intern. Med.* **29**: 1036–1044. [Medline] [CrossRef]

30. Nicolle, A. P., Chetboul, V., Allerheiligen, T., Pouchelon, J. L., Gouni, V., Tessier-Vetzel, D., Sampedrano, C. C. and Lefebvre, H. P. 2007. Azotemia and glomerular filtration rate in dogs with chronic valvular disease. *J. Vet. Intern. Med.* **21**: 943–949. [Medline] [CrossRef]

31. Onogawa, T., Sakamoto, Y., Nakamura, S., Nakayama, S., Fujiki, H. and Yamamura, Y. 2011. Effects of tolvaptan on systemic and renal hemodynamic function in dogs with congestive heart failure. *Cardiovasc. Drugs Ther.* **25** Suppl 1: S67–S76. [Medline] [CrossRef]

32. Prekker, M. E., Scott, N. L., Hart, D., Sprenkle, M. D. and Leatherman, J. W. 2013. Point-of-care ultrasound to estimate central venous pressure: a comparison of three techniques. *Crit. Care Med.* **41**: 833–841. [Medline] [CrossRef]

33. Raja, K., Kochhar, R., Sethy, P. K., Dutta, U., Bali, H. K. and Varma, J. S. 2004. An endoscopic study of upper-GI mucosal changes in patients with congestive heart failure. *Gastrointest. Endosc.* **60**: 887–893. [Medline] [CrossRef]

34. Ronco, C., Cicoira, M. and McCullough, P. A. 2012. Cardiorenal syndrome type 1: pathophysiological crosstalk leading to combined heart and kidney dysfunction in the setting of acutely decompensated heart failure. *J. Am. Coll. Cardiol.* **60**: 1031–1042. [Medline] [CrossRef]

35. Rudski, L. G., Lai, W. W., Afilalo, J., Hua, L., Handschumacher, M. D., Chandrasekaran, K., Solomon, S. D., Louie, E. K. and Schiller, N. B. 2010. Guidelines for the echocardiographic assessment of the right heart in adults: a report from the American Society of Echocardiography endorsed by the European Association of Echocardiography, a registered branch of the European Society of Cardiology, and the Canadian Society of Echocardiography. *J. Am. Soc. Echocardiogr.* **23**: 685–713, quiz 786–788. [Medline] [CrossRef]

36. Saleh, N., Aoki, M., Shimada, T., Akiyoshi, H., Hassanin, A. and Ohashi, F. 2005. Renal effects of medetomidine in isoflurane-anesthetized dogs with special reference to its diuretic action. *J. Vet. Med. Sci.* **67**: 461–465. [Medline] [CrossRef]

37. Sandek, A., Swidsinski, A., Schroedl, W., Watson, A., Valentova, M., Herrmann, R., Scherbakov, N., Cramer, L., Rauchhaus, M., Grosse-Herrenthey, A., Krueger, M., von Haehling, S., Doehner, W., Anker, S. D. and Bauditz, J. 2014. Intestinal blood flow in patients with chronic heart failure: a link with bacterial growth, gastrointestinal symptoms, and cachexia. *J. Am. Coll. Cardiol.* **64**: 1092–1102. [Medline] [CrossRef]

38. Schneider, A. G., Hofmann, L., Wuerzner, G., Glatz, N., Maillard, M., Meuwly, J. Y., Eggimann, P., Burnier, M. and Vogt, B. 2012. Renal perfusion evaluation with contrast-enhanced ultrasonography. *Nephrol. Dial. Transplant.* **27**: 674–681. [Medline] [CrossRef]

39. Shinbane, J. S., Wood, M. A., Jensen, D. N., Ellenbogen, K. A., Fitzpatrick, A. P. and Scheinman, M. M. 1997. Tachycardia-induced cardiomyopathy: a review of animal models and clinical studies. *J. Am. Coll. Cardiol.* **29**: 709–715. [Medline] [CrossRef]

40. Takeda, K., Kimura, K. and Sato, A. 2007. Diagnosis of acute necrotizing pancreatitis by perfusion CT. *Suizo* **22**: 547–555. [CrossRef]

41. Takeda, K., Mikami, Y., Fukuyama, S., Egawa, S., Sunamura, M., Ishibashi, T., Sato, A., Masamune, A. and Matsuno, S. 2005. Pancreatic ischemia associated with vasospasm in the early phase of human acute necrotizing pancreatitis. *Pancreas* **30**: 40–49. [Medline]

42. Tanaka, T., Ichiba, Y., Miura, Y., Koide, K., Matsugu, Y., Kodo, Y., Fujii, T., Ito, H. and Dohi, K. 1997. [Histopathological study in models of chronic pancreatitis]. *Nihon Shokakibyo Gakkai Zasshi* **94**: 739–745 (in Japanese). [Medline]

43. Trivedi, S., Marks, S. L., Kass, P. H., Luff, J. A., Keller, S. M., Johnson, E. G. and Murphy, B. 2011. Sensitivity and specificity of canine pancreas-specific lipase (cPL) and other markers for pancreatitis in 70 dogs with and without histopathologic evidence of pancreatitis. *J. Vet. Intern. Med.* **25**: 1241–1247. [Medline] [CrossRef]

44. Wilson, J. R., Douglas, P., Hickey, W. F., Lanoce, V., Ferraro, N., Muhammad, A. and Reichek, N. 1987. Experimental congestive heart failure produced by rapid ventricular pacing in the dog: cardiac effects. *Circulation* **75**: 857–867. [Medline] [CrossRef]

45. Winton, F. R. 1931. The influence of venous pressure on the isolated mammalian kidney. *J. Physiol.* **72**: 49–61. [Medline] [CrossRef]